Effective Defect Classification for Flat Display Panel Film Images[1]

Chung-Ho Noh
School of Industrial and Management Eng., Hankuk University of Foreign Studies
82-31-330-4512
nochu@hufs.ac.kr

Seok-Lyong Lee
School of Industrial and Management Eng., Hankuk University of Foreign Studies
82-31-330-4357
sllee@hufs.ac.kr

Deok-Hwan Kim
School of Electronics Engineering, Inha University
82-32-860-7424
deokhwan@inha.ac.kr

Chin-Wan Chung
Computer Science, College of Information & Science Technology, KAIST
82-42-869-3537
chungcw@kaist.edu

ABSTRACT
In this paper, we propose an effective defect classification system for FDP (flat display panel) film images which are acquired in real production lines. A film image is segmented into a binary image with two non-overlapping regions: defect and non-defect regions. From the defect regions, various features are extracted such as brightness distribution, linearity, and morphologic characteristics. The film defects are classified through the analysis of those features extracted. Empirical study shows our system classifies five types of film defects effectively.

Keywords
Defect classification, Flat display panel, Image analysis, Shape descriptor.

1. INTRODUCTION
A flat display panel is used in various display devices such as LCD (liquid crystal display), PDP (plasma display panel), and LED (light emitting diode), and is becoming popular since it is widely used in a variety of electronic devices, like digital watches, measuring instruments, and mobile devices. There has been excessive competition in the FDP industry, and companies are making great efforts to increase their market share.

It is important to produce high-quality products and enhance productivity in the panel display production in order to strengthen the competitiveness of their commodities on related markets.

Various defects are generated during the process of attaching films to the panel at the production line. The accurate and timely detection of these defects is crucial process. In order to detect those defects, it is essential to use an automated defect inspection system since the panel moves fast along the production line and some defects are too small to be recognized by the human eye. The defect inspection is divided into two sub-processes: defect detection and defect classification. Most studies have focused on the former while only few researches have been made for the latter. As the quality and productivity issues are critical, the accurate classification is becoming important since engineers can handle defects properly depending on the types.

Although the defect inspection is becoming important, a few literatures have been published since most companies consider the inspection as confidential. As a recent work, Lu and Tsai [5] extracted defect regions using the singular value decomposition. They determined defect regions by eliminating the orthogonal components and re-building the image. However it causes considerable overheads in decomposing and reconstructing a defect image. There are researches that use well-known approach, an adaptive threshold technique. Kim et al. [3] used the statistical characteristics of local blocks and pattern elimination techniques based on the pixel difference and adaptive multilevel threshold technique. Oh et al. [7] used a directional filter bank (DFB) and an adaptive multilevel threshold technique to find line-type defects in TFT-LCD panels. These methods are fast but they have a weakness in that it identifies only specific types (spot and line types) of defects, preventing it from being applied for diverse applications.

There are considerable researches [1, 2, 4] that focused on classifying a non-uniformity defect, known as mura. They quantized and detected mura using a polynomial approximation [1], an analysis of the variance [2], and modified regression diagnostics and thresholds [4], respectively. However, these methods focused on detection without considering classification. In order to classify multiple defect types, Yoon et al. [8] proposed a classification method that exploited region-growing based segmentation using a gray level co-occurrence matrix. They classified micro defects that needed to be magnified before processing. But, it degrades the runtime efficiency considerably.

In this paper, we present an effective defect classification system for FDP film images which are acquired in LCD and PDP production lines. Using statistical techniques and adaptive

[1]This work was supported by Defense Acquisition Program Administration and Agency for Defense Development under the contract UD030000AD. Corresponding author: Seok-Lyong Lee (sllee@hufs.ac.kr)

ICHIT'09, August 27–29, 2009, Daejeon, Korea.

methods, a film image is segmented into a binary image which has two non-overlapping regions: defect and non-defect regions. From the defect regions, various features are extracted such as brightness distribution, linearity, and morphologic characteristics. Our system is designed to classify five types of defects, i.e., hollows, craters, scratches, black spots, and water bubbles, through the analysis of those features extracted.

2. PROPOSED WORK

2.1 Binary Image Generation

From a defect image, a binary image is generated to detect and quantize defects. It is important to determine a threshold that distinguishes defects from the background of the image. We use a statistical method to get the threshold using a mean (μ_b) and standard deviation (σ_b) of the background. Exploiting a control chart, each pixel is evaluated whether it is included in a defect region or not. Thus, we get an adaptive threshold, $\mu_b \pm k\sigma_b$, since μ_b and σ_b vary according to the brightness of background, as follows:

$$I'(x,y) = \begin{cases} 0, & when\ \mu_b - k\sigma_b \le I(x,y) \le \mu_b + k\sigma_b, \\ 255, & otherwise. \end{cases} \quad (1)$$

In Equation (1), $I(x, y)$ and $I'(x, y)$ are the intensities of pixels at (x, y) of the original and binary image, respectively. k is a parameter to compute a threshold for the defect region and is determined empirically. Figure 1 shows original film images and corresponding binary images using a statistical method.

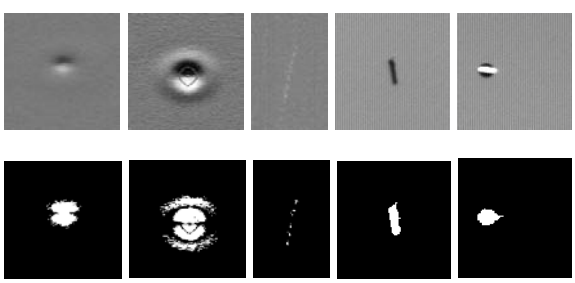

(a) (b) (c) (d) (e)

Figure 1. Original FT-LCD film images and corresponding binary images using an adaptive threshold method, $\mu_b \pm k\sigma_b$: (a) hollow, (b) crater, (c) scratch, (d) black spot, (e) water bubble

2.2 Feature Extraction

2.2.1 Linear fitting

The linear fitting (LF) is used to evaluate the linear characteristics of a defect. It is useful to classify line-type defects such as scratches. First, an equation of the first degree of a line is derived such that the line might fit in with the distribution of pixels in a defect region. Let (x_i, y_i) be rectangular coordinates of pixel p_i $(1 \le i \le u)$. Then the equation of a line is as follows:

$$\begin{bmatrix} 1 & x_1 \\ 1 & x_2 \\ \vdots & \vdots \\ 1 & x_u \end{bmatrix} \begin{bmatrix} C \\ D \end{bmatrix} = \begin{bmatrix} y_1 \\ y_2 \\ \vdots \\ y_u \end{bmatrix}$$

$$\bar{y} = C\bar{x} + D \quad (2)$$

The distance between pixel p_i and the line derived from Equation (2) is calculated. The distribution of these distances represents the linear property of a defect and LF is computed as follows:

$$LF = \frac{V_{d(i,i')}}{\max(d(i,j))} \quad (3)$$

where $d(i, j)$ is the distance between p_i and p_j $(1 \le i,j \le u)$, $i' = \arg\min_{l \in L} d(i,l)$, where L is a set of pixels on the line derived from equation (2), and V is the variance with respect to $d(i, l)$. A defect tends to be line-types as LF decreases.

2.2.2 Multi-level intensity ratio

When a film defect does not have any specific shape, it is difficult to apply the linear fitting. For these non-uniformity defects, we propose the multi-level intensity ratio (MIR) that represents the distribution for a specific range of intensity values. We construct an intensity ratio histogram (*IR*), each bin of which contains a ratio of a specific intensity range with respect to the whole intensity, as follows:

$$IR_A(t) = \#\{p : I(p) = t, p \in DR\} \quad (4)$$

Where A is a defect image, t is a specific intensity value $(0 \le t \le 255)$, $I(p)$ is an intensity of pixel p, and DR is a set of pixels in a defect region of A. Figure 2 shows a defect image and its intensity ratio histogram.

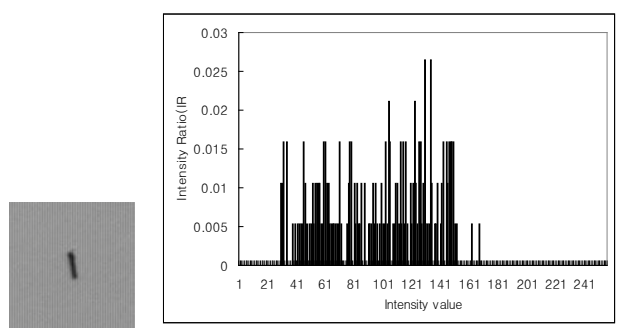

(a) (b)

Figure 2. A defect images (a) and its intensity ratio histogram (b)

To simplify and speed up the process, we quantize the intensity depending on application requirements. We introduce a parameter m that represents the level of quantization. For example, the histogram has 256 bins, a bin for each intensity value when $m = 1$, and it has 4 bins (0-63, 64-127, 128-191, and 192-255) when $m = 7$. Using the multi-level intensity ratio histogram, the similarity, $sim_{MIR}(A, B)$, between two defect images, A and B, is defined as follows:

$$sim_{MIR}(A,B) = \frac{\left(\frac{1}{2} \sum_{n=1}^{m} \sum_{k=1}^{\frac{256}{2^{n-1}}} \frac{\left(\sum_{i=2^{n-1}(k-1)+1}^{2^{n-1}k} IR_A(i) - \sum_{i=2^{n-1}(k-1)+1}^{2^{n-1}k} IR_B(i) \right)^2}{\sum_{i=2^{n-1}(k-1)+1}^{2^{n-1}k} IR_A(i) + \sum_{i=2^{n-1}(k-1)+1}^{2^{n-1}k} IR_B(i)} \right)}{m} \quad (5)$$

By considering the *multi*-level intensity, we can identify film defects at diverse levels of granularity, from detail to overall intensity distribution. In this paper, we consider 7 levels of quantization (m=1 through 7) at the same time.

2.2.3 Shape context

For the shape identification of defects, we use the shape context [6], in which a shape is represented by a set of points, $P = \{p_1, \ldots, p_n\}$, $p_i \in R^2$ of n points, that are sampled from the contours on the shape. For a point p_i on the shape, a histogram h_i of the relative coordinates of the remaining n-1 points is defined as the *shape context* of p_i and is expressed as follows:

$$h_i(k) = \#\{q \neq p_i : (q - p_i \in bin(k))\} \quad (6)$$

In the above equation, $bin(k)$ is the kth bin of h_i. Consider the insect image in Figure 3(a). A log-polar coordinate system with 5x12 bins is shown in Figure 3(b), where random sample points were chosen from edge points and median distance λ for all N^2 point pairs is shown for reference. Figure 3(c) gives an example of the log r, θ histogram where the dark bins denote larger values.

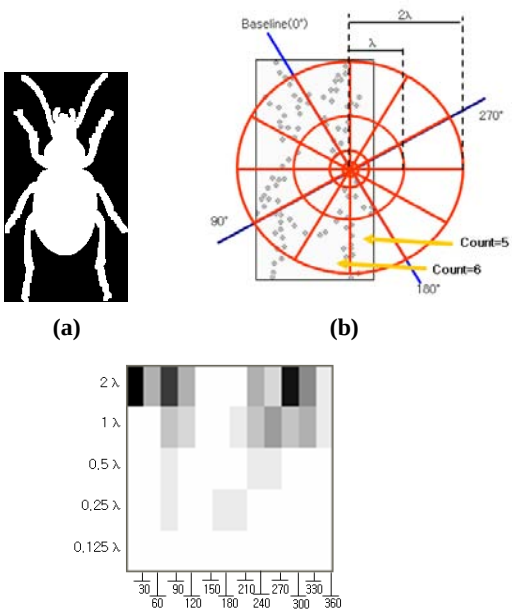

(a) **(b)**

(c)

Figure 3. Log-polar histogram: (a) An insect image (b) Diagram of log-polar histogram with 5x6 bins (c) log r, θ histogram

The matching cost, C_s, of two defects is computed from the shape context and is given by the χ^2 distance between the two corresponding histograms. Let the two histograms be denoted by $h_i(k)$ and $h_j(k)$ respectively. Then, C_s can be computed as follows:

$$C_S = \frac{1}{2} \sum_{k=1}^{K} \frac{[h_i(k) - h_j(k)]^2}{h_i(k) + h_j(k)} \quad (7)$$

2.3 Defect Classification

To determine the type of a defect, a binary image for each defect is produced as described in Section 3.1. Line-typed defects such as scratches are first discriminated using the linear fitting method. A defect is regarded as line-typed if LF≤TH_{LF}, where TH_{LF} is a threshold that is determined empirically. In determining other types of defects, a template database is used, where feature values of referential defects are stored. We have chosen a set of representative defects for each type according to domain experts' recommendation. For classifying the non-uniformity defects such as black spots and water bubbles, the multi-level intensity ratio is used. A defect is considered as the same as that of the best matched referential defect in the database. If the similarity between a defect and a referential defect is larger than a threshold (TH_{MIR}), then the defect is assumed to be another type. Finally, for defects with comparatively clear shapes like hollows and craters, the shape context is used. When a defect is to be evaluated, the shape feature of the defect is extracted, and the matching cost between the defect and referential defects in a template database is computed. The defect type is determined by matching a defect to a referential image whose matching cost with respect to the defect is the smallest among all template images in the database. If the given defect is not matched to any referential defect in the database (i.e. the minimum cost is larger than a specified threshold TH_{SH}), it is regarded as an *unknown* type.

3. EXPERIMENTS AND CONCLUDING REMARKS

To evaluate the effectiveness of our proposed method, we have implemented a defect inspection system using MS Visual C++ under a Xeon 2.5GHz Dual CPU Server.

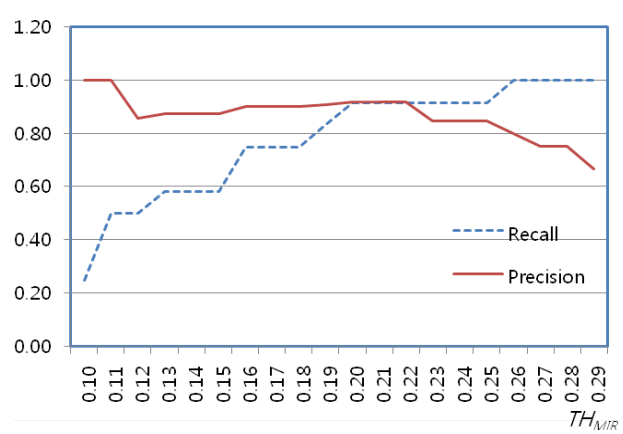

Figure 4. Precision and recall with respect to TH_{MIR} for non-uniformity defects. The most effective result is observed when TH_{MIR} = 0.21.

An experimental data set consists of 70 defect images including 19 scratches, 7 black spots, 5 water bubbles, 15 hollows, 18 craters, and 6 unknown defects. We need to determine thresholds for the defect classification using separate data sets. The threshold

values TH_{LF}, TH_{MIR}, and TH_{SH} are empirically chosen to be 0.03, 0.21, and 0.27, respectively. Due to the space limitation, we do not include all processes that determine those thresholds. Instead, we give an example for TH_{MIR}. Figure 4 shows the precision and recall with respect to non-uniformity defects using MIR. We can observe that TH_{MIR} = 0.21 produces the most effective result (*precision*=0.9, *recall*=0.9). Table 1 shows the final experimental results on classifying defect types. As we can see from the table, most of defects are correctly classified. The recall is in the range 0.67-1.0 and on the average 0.90 while the precision is in the range 0.71-1.0 and on the average 0.90. These results come up to our expectations and we believe our method is applicable in related industries.

Table 1. Experimental results with respect to the classification of defect types

		Defect type						Total
		Scra-tch	Black spot	Water bubble	Hol-low	Crater	Un-known	
Ground Truth		19	7	5	15	18	6	70
Res-sult	Correct	19	6	5	10	18	5	63
	In-correct	0	1	0	0	4	2	7
Precision		1	0.86	1	1	0.82	0.71	0.90
Recall		1	0.86	1	0.67	1	0.83	0.90

In this paper we proposed an effective defect classification system that is used in the last stage of flat display panel manufacturing. We used three features in determining defect types: linear fitting, multi-level intensity ratio, and shape context. Using those features we were able to classify five frequently-occurred defects effectively. An application that is emphasized in this paper is the classification of film defects, but we believe other potential inspection areas, such as flaw detection over glass surfaces, vessels, and various types of films, can also benefit from the research.

4. ACKNOWLEDGMENTS

This work was supported by Defense Acquisition Program Administration and Agency for Defense Development under the contract UD030000AD. Our thanks to CasaTech Inc. for providing us with a set of film defect images for the experiment.

5. REFERENCES

[1] Baek S. I., Kim W. S., Koo T. M., Choi I. & Park K. H., Inspection of defect on LCD panel using polynomial approximation. In: Proceedings of IEEE Region 10 Conference, Vol .1, 2004, 235-238.

[2] Jiang B. C., Wang C. C. & Liu H. C., Liquid crystal display surface uniformity defect inspection using analysis of variance and exponentially weighted moving average techniques. International Journal of Production Research, 43(1), 2005, 67-80.

[3] Kim W. S., Kwak D. M., Song Y. C., Choi D. H. & Park K. H., Detection of Spot-Type Defects on Liquid Crystal Display Modules. Key Engineering Materials, Vol. 270-273, 2004, 808-813.

[4] Lee J. Y. & Yoo S. I., Automatic Detection of Region-Mura Defect in TFT-LCD. IEICE TRANS. INF. & SYSE, E87-D(10), 2004, 2371-2378.

[5] Lu C. J. and Tsai D. M., "Defect inspection of patterned thin film transistor-liquid crystal display panels using a fast sub-image-based singular value decomposition." International Journal of Production Research, Vol. 42, No. 20, 2004, pp. 4331-4351.

[6] Mori G., Belongie S. & Malik J., Efficient shape matching using shape contexts. IEEE Transactions on Pattern Analysis and Machine Intelligence, 27(11), 2005, 1832-1837.

[7] Oh J. H., Kwak D. M., Lee K. B., Song Y. C., Choi D. H. & Park K. H., Line Defect Detection in TFT-LCD Using Directional Filter Bank and Adaptive Multilevel Thresholding. Key Engineering Materials, Vol. 270-273, 2004, 233-238.

[8] Yoon Y. G., Lee S. L., Chung C. W. & Kim S. H., An effective defect inspection system for polarized film images using image segmentation and template matching techniques. Computers & IE, 55(3), 2008, 567-583.